Central role of mic10 in the mitochondrial contact site and cristae organizing system

Bohnert, Maria; Zerbes, Ralf M; Davies, Karen M; Mühleip, Alexander W; Rampelt, Heike; Horvath, Susanne E; Boenke, Thorina; Kram, Anita; Perschil, Inge; Veenhuis, Marten

Published in:
Cell metabolism

DOI:
10.1016/j.cmet.2015.04.007

Publication date:
2015

Cell Metabolism
Short Article

Central Role of Mic10 in the Mitochondrial Contact Site and Cristae Organizing System

Maria Bohnert,[1] Ralf M. Zerbes,[1,2] Karen M. Davies,[3] Alexander W. Mühleip,[3] Heike Rampelt,[1] Susanne E. Horvath,[1] Thorina Boenke,[1] Anita Kram,[4] Inge Perschil,[1] Marten Veenhuis,[4] Werner Kühlbrandt,[3] Ida J. van der Klei,[4] Nikolaus Pfanner,[1,5,*] and Martin van der Laan[1,5,*]
[1]Institut für Biochemie und Molekularbiologie, ZBMZ, Universität Freiburg, 79104 Freiburg, Germany
[2]Faculty of Biology, Universität Freiburg, 79104 Freiburg, Germany
[3]Department of Structural Biology, Max Planck Institute of Biophysics, 60438 Frankfurt am Main, Germany
[4]Molecular Cell Biology, University of Groningen, 9700 CC Groningen, the Netherlands
[5]BIOSS Centre for Biological Signalling Studies, Universität Freiburg, 79104 Freiburg, Germany
*Correspondence: nikolaus.pfanner@biochemie.uni-freiburg.de (N.P.), martin.van.der.laan@biochemie.uni-freiburg.de (M.v.d.L.)
http://dx.doi.org/10.1016/j.cmet.2015.04.007

SUMMARY

The mitochondrial contact site and cristae organizing system (MICOS) is a conserved multi-subunit complex crucial for maintaining the characteristic architecture of mitochondria. Studies with deletion mutants identified Mic10 and Mic60 as core subunits of MICOS. Mic60 has been studied in detail; however, topogenesis and function of Mic10 are unknown. We report that targeting of Mic10 to the mitochondrial inner membrane requires a positively charged internal loop, but no cleavable presequence. Both transmembrane segments of Mic10 carry a characteristic four-glycine motif, which has been found in the ring-forming rotor subunit of F_1F_o-ATP synthases. Overexpression of Mic10 profoundly alters the architecture of the inner membrane independently of other MICOS components. The four-glycine motifs are dispensable for interaction of Mic10 with other MICOS subunits but are crucial for the formation of large Mic10 oligomers. Our studies identify a unique role of Mic10 oligomers in promoting the formation of inner membrane crista junctions.

INTRODUCTION

The mitochondrial inner membrane consists of two main domains: the inner boundary membrane located close to the outer membrane and the cristae membranes that form deep invaginations. The relatively narrow connections between inner boundary membrane and cristae membranes are termed crista junctions (Frey and Mannella, 2000; Zick et al., 2009; van der Laan et al., 2012). Preprotein translocases are enriched in the inner boundary membrane, whereas respiratory chain complexes are enriched in cristae membranes (Vogel et al., 2006). Various factors have been described that are involved in the formation or maintenance of inner membrane architecture, including the fusion protein Mgm1/OPA1 and the F_1F_o-ATP synthase, which is located at crista rims (Paumard et al., 2002; Frezza et al., 2006; Meeusen et al., 2006; Merkwirth et al., 2008; Strauss et al., 2008; Davies et al., 2012).

A large protein complex was found to be enriched at crista junctions. The complex is termed the mitochondrial contact site and cristae organizing system (MICOS; previously termed MINOS or MitOS) (Rabl et al., 2009; Harner et al., 2011; Hoppins et al., 2011; von der Malsburg et al., 2011; Alkhaja et al., 2012; Jans et al., 2013). Six subunits of the MICOS complex have been identified, termed Mic10 to Mic60 (Pfanner et al., 2014). All subunits are inner membrane proteins exposed to the intermembrane space. Mic19 is a peripheral membrane protein, whereas all other MICOS subunits contain at least one hydrophobic transmembrane segment (Harner et al., 2011; Hoppins et al., 2011; von der Malsburg et al., 2011; Alkhaja et al., 2012; van der Laan et al., 2012). Mutant cells lacking Mic10 or Mic60 display a dramatically altered cristae structure. Most crista junctions are lost; the cristae are detached from the inner boundary membrane and form large internal membrane stacks (John et al., 2005; Rabl et al., 2009; Mun et al., 2010; Head et al., 2011; Harner et al., 2011; Hoppins et al., 2011; von der Malsburg et al., 2011; Alkhaja et al., 2012). Mutant cells lacking Mic12, Mic19, or Mic27 show principally similar but less severe morphological alterations (Darshi et al., 2011; Harner et al., 2011; Head et al., 2011; Hoppins et al., 2011; von der Malsburg et al., 2011; Weber et al., 2013). Cells lacking Mic26, which is homologous to Mic27, show only minor morphological alterations.

Based on the severe mutant phenotypes, Mic10 and Mic60 are considered to represent the two core components of MICOS. Mic60 (mitofilin/Fcj1) is targeted to mitochondria by an N-terminal cleavable presequence and is anchored in the inner membrane by a single transmembrane segment at the N terminus (Rabl et al., 2009). The major portion of Mic60 is located in the intermembrane space and forms contact sites with several outer membrane proteins, including the protein translocase of the outer membrane (TOM), the sorting and assembly machinery (SAM), the fusion protein Ugo1, and porin (VDAC) (Xie et al., 2007; Darshi et al., 2011; Harner et al., 2011; Hoppins et al., 2011; von der Malsburg et al., 2011; Bohnert et al., 2012; Körner et al., 2012; Ott et al., 2012; Zerbes et al., 2012a). The interaction of Mic60 with TOM is important to promote translocation of precursor proteins into the intermembrane

space and the outer membrane (von der Malsburg et al., 2011; Bohnert et al., 2012).

Little is known about topogenesis and function of Mic10 (Mio10/Mcs10/Mos1/MINOS1). Different views have been reported about its topology in the inner membrane (Harner et al., 2011; Hoppins et al., 2011; von der Malsburg et al., 2011; Alkhaja et al., 2012; van der Laan et al., 2012). In each model, only short segments of Mic10 are located in the intermembrane space, and no evidence for a direct interaction of Mic10 with outer membrane components has been found. It is unknown why the lack of Mic10 leads to strong alterations of inner membrane morphology.

We observed that Mic10 not only interacts with the other MICOS subunits but also forms large oligomers. The transmembrane segments of Mic10 contain conserved glycine motifs that are crucial for homo-oligomerization but not for the interaction with other MICOS subunits. Overexpression of Mic10 strongly increases the abundance of Mic10 oligomers, which leads to a considerable extension and deformation of cristae membranes and crista junctions. Our findings suggest a central role of Mic10 for mitochondrial inner membrane architecture and generation of crista junctions.

RESULTS AND DISCUSSION

Overexpression of Mic10 Alters Inner Membrane Architecture

So far, the function of Mic10 has been studied in deletion mutants; however, the levels of Mic27 (Aim37/Mcs27) are strongly reduced in *mic10*Δ cells (Harner et al., 2011; Hoppins et al., 2011; von der Malsburg et al., 2011). To study if the lack of Mic10 alone leads to the characteristic alterations of inner membrane morphology, we generated a *mic10*Δ yeast strain that expressed Mic27 from a high-copy-number plasmid (Figure 1A). Restoration of Mic27 levels did not change the *mic10*Δ phenotype (Figure 1B), demonstrating that Mic10 itself is crucial for maintaining the shape of the inner membrane.

Mic10 was overexpressed in budding yeast. The mitochondrial levels of Mic10 were increased ~4-fold, whereas the levels of other MICOS subunits including Mic27 remained close to the wild-type range (Figure 1C). In electron micrographs of cell sections, Mic10↑ mitochondria displayed a distinctive phenotype with considerably elongated and deformed cristae (Figure 1D). Mic60↑ cells showed a different mitochondrial ultrastructure with an increased branching of cristae (Rabl et al., 2009). Overexpression of other MICOS subunits did not lead to characteristic morphological alterations (Figure 1D; Figure S1 available online). Thus, the two MICOS subunits that show the strongest phenotypes in deletion mutants lead to characteristic but distinct morphological alterations upon overexpression.

Characteristic Motifs and Targeting of Mic10

Mic10 is an integral protein of the inner membrane that has been conserved in evolution (Zerbes et al., 2012b). Both predicted transmembrane segments contain a conserved motif with multiple glycines, typically GxGxGxG (Figure 2A). Such a motif has been found in the first transmembrane segment of the ring-forming subunit c of F_1F_o-ATP synthases (Vonck et al., 2002; Alavian et al., 2014). In addition, the short predicted loop between the Mic10 transmembrane segments is highly positively charged (Figure 2A).

Different views have been reported about the number of transmembrane segments and the inner membrane topology of Mic10. In contrast to the model with two transmembrane segments (von der Malsburg et al., 2011; Alkhaja et al., 2012; Figure 2A), Harner et al. (2011) predicted that Mic10 contains only one transmembrane segment and thus would expose its N terminus into the matrix. We generated yeast strains that expressed Mic10 with a hemagglutinin (HA) tag at either N terminus or C terminus. Upon opening of the mitochondrial intermembrane space by osmotic swelling, protease treatment of the resulting mitoplasts generated a characteristic fragment of wild-type Mic10 (Figure 2B, lane 4). Upon protease treatment of mitoplasts, each HA tag was removed and the characteristic Mic10′ fragment was generated like in wild-type (Figure 2B). Thus, Mic10 exposes both termini to the intermembrane space, supporting the view that it spans the inner membrane twice.

The N-terminal segment of Mic10 does not resemble a positively charged presequence. Upon import of the radiolabeled Mic10 precursor into mitochondria, no proteolytic processing was observed (Figure 2C). We asked if the positively charged loop of Mic10 was critical for targeting of the protein to mitochondria and generated a yeast strain where the positively charged cluster was replaced by alanine residues. Mitochondria isolated from this strain contained Mic10, although in a moderately reduced amount, whereas the level of Mic27 was drastically reduced like in *mic10*Δ mitochondria (Figure 2D). The inner membrane cristae structure was strongly altered like in *mic10*Δ yeast (Figure 2E). We fractionated the yeast cells and found a dual localization of the mutant form of Mic10. A considerable amount of the Mic10 molecules lacking the positively charged loop were found in the microsomal fraction that includes the endoplasmic reticulum (Figure 2F). The remaining mitochondria-located mutant Mic10 was accessible to added protease in intact mitochondria, leading to generation of the Mic10′ fragment, which in wild-type mitochondria is formed only after opening of the intermembrane space (Figure 2G, lanes 4 and 7). Protease treatment of microsomes generated a similar fragment (Figure 2G, lane 12). Mic10 lacking the positively charged loop is thus accessible to protease from the cytosolic side both in mitochondria and microsomes, demonstrating that it was mistargeted to the mitochondrial outer membrane and the microsomal fraction. In addition, we generated a yeast strain where the conserved proline residue in the second transmembrane segment was replaced by alanine, yet did not observe characteristic alterations in this mutant (Figures S2A–S2C).

We conclude that Mic10 spans the inner membrane twice and exposes both termini to the intermembrane space. The matrix-exposed positively charged loop connecting both transmembrane segments is required for targeting of Mic10 into the inner membrane. In addition, the stability of Mic27 depends on inner membrane-located Mic10.

Role of Mic10 in the Organization of the MICOS Complex

Glycine motifs in transmembrane segments are known to promote protein-protein interactions (Russ and Engelman, 2000; Senes et al., 2004). We performed an in organello crosslinking approach using a homo-bifunctional amino-reactive crosslinking

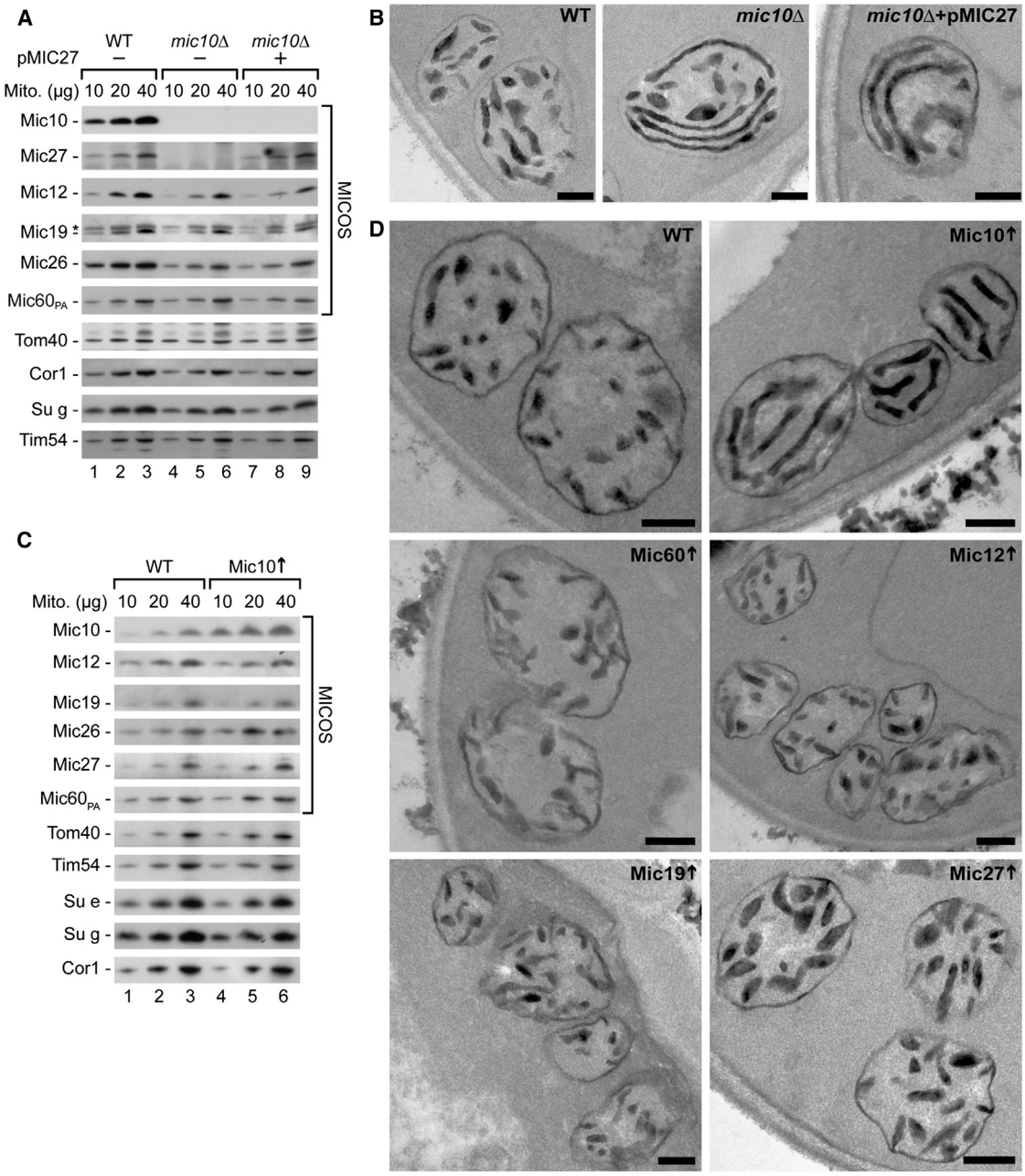

Figure 1. Overexpression of Mic10 Affects Mitochondrial Ultrastructure

(A) Protein levels of wild-type (WT), *mic10*Δ, and *mic10*Δ pMIC27 ($Mic60_{ProtA(PA)}$) mitochondria analyzed by SDS-PAGE and immunoblotting. μg, total mitochondrial protein; asterisk, unspecific band.

(B) Representative EM images of mitochondria from the indicated yeast strains using DAB staining. Bar, 200 nm.

(C) Protein levels of mitochondria from WT and Mic10-overexpressing cells ($Mic60_{ProtA}$) analyzed as in (A).

(D) Representative DAB-stained images of mitochondria from WT cells and cells overexpressing the indicated MICOS subunits. Bar, 200 nm.

See also Figure S1 and Table S1.

reagent. We found that Mic10 was in close proximity to all other MICOS subunits (Figure S3), underscoring its central role in the MICOS complex. Mic10 and Mic60 are required for the stability of the MICOS complex (Harner et al., 2011; Hoppins et al., 2011; von der Malsburg et al., 2011). To differentiate between the roles of Mic10 and Mic60 in MICOS organization, we attached affinity tags to other MICOS subunits and deleted either *MIC10* or *MIC60*. (1) Tagged Mic19 pulled down the MICOS subunits from digitonin-lysed mitochondria. When *MIC60* was deleted, however, Mic19 did not pull down any other MICOS subunits (Figure 3A), indicating that the association of Mic19 with MICOS depends on Mic60. Upon deletion of

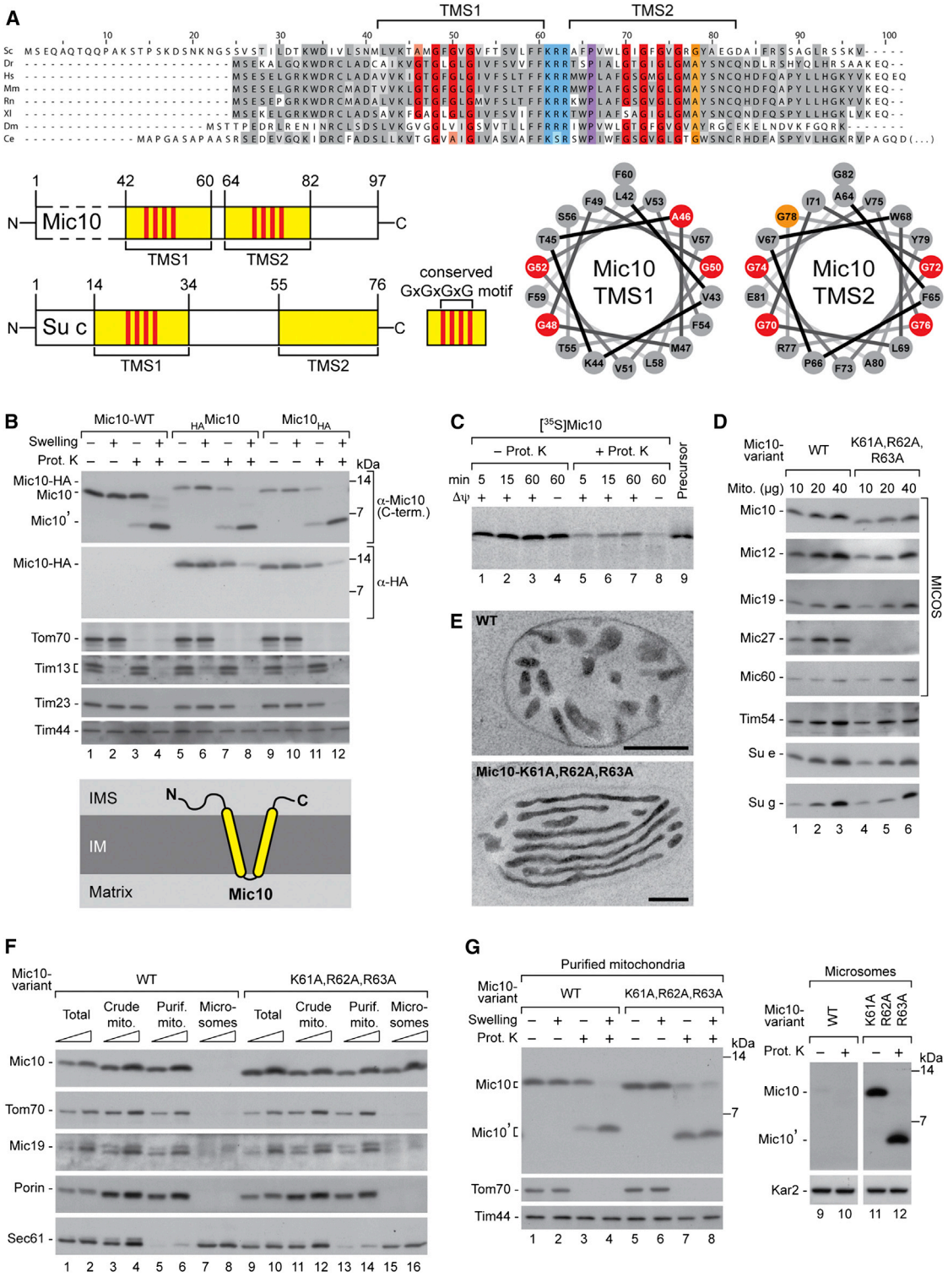

Figure 2. Topology and Targeting of Mic10 to the Mitochondrial Inner Membrane

(A) Top: Alignment of Mic10 sequences from *S. cerevisiae* (Sc), *D. rerio* (Dr), *H. sapiens* (Hs), *M. musculus* (Mm), *R. norvegicus* (Rn), *X. laevis* (Xl), *D. melanogaster* (Dm), and *C. elegans* (Ce). TMS, transmembrane segments; red, glycine motifs; blue, positively charged loop; violet, conserved proline; gray, identical residues; light gray, similar residues. Bottom left: Domain structures of *S. cerevisiae* Mic10 and F_1F_o ATP synthase subunit c. Bottom right: Helical wheel projections of Mic10 TMS1 and TMS2.

(B) WT, $_{HA}$Mic10, and Mic10$_{HA}$ mitochondria were subjected to hypo-osmotic swelling and proteinase K treatment (Prot. K) as indicated. Mic10′, Prot. K-generated fragment of membrane-embedded Mic10. Bottom: Deduced topology of Mic10.

(legend continued on next page)

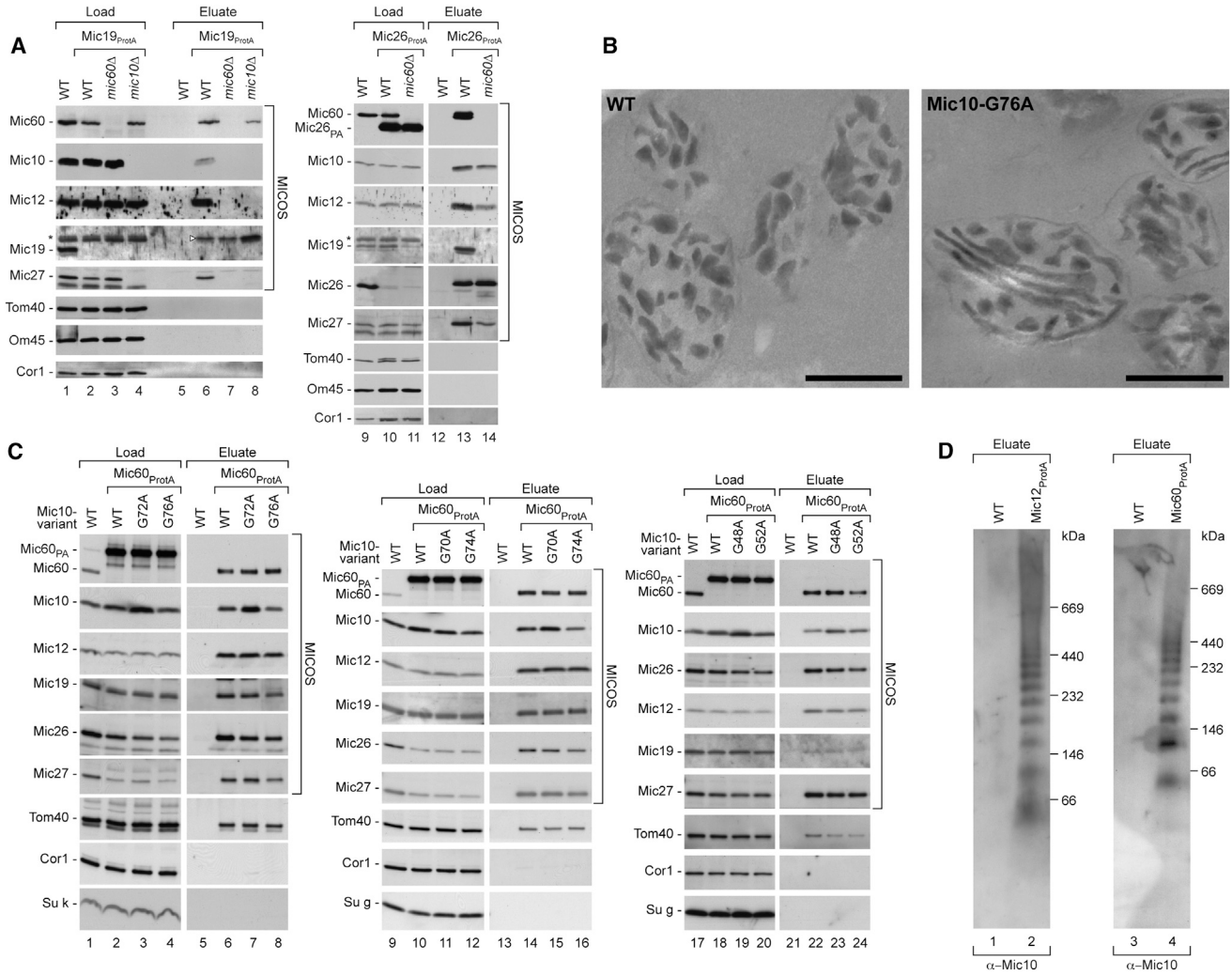

Figure 3. Identification of MICOS Subcomplexes and Mic10 Oligomers

(A) Mitochondria were solubilized with digitonin and incubated with IgG Sepharose beads. After elution of bound proteins with TEV protease, samples were analyzed by SDS-PAGE and immunoblotting. Load 4%; eluate 100%. Asterisk, unspecific band; arrowhead, TEV-cleaved $Mic19_{ProtA}$.

(B) Representative EM images of mitochondria in WT and $Mic10^{G76A}$ cells visualized by DAB staining. Bar, 500 nm.

(C) Mitochondria isolated from WT and $Mic60_{ProtA}$ cells expressing the indicated Mic10 variants were subjected to affinity chromatography and analyzed as in (A).

(D) WT, $Mic12_{ProtA}$, and $Mic60_{ProtA}$ mitochondria were treated as described in (A). Eluates were analyzed by blue native PAGE and immunoblotting.

See also Figure S3 and Table S1.

MIC10, Mic19 pulled down Mic60 molecules, but none of the other MICOS subunits. Together with the observation that in *mic60*Δ mitochondria, the level of (untagged) Mic19 is strongly decreased (Harner et al., 2011; Hoppins et al., 2011; von der Malsburg et al., 2011), these findings reveal a close interaction of Mic19 with Mic60. (2) Tagged Mic26 efficiently pulled down all MICOS subunits. Upon deletion of *MIC60*, Mic26 still pulled down all other MICOS subunits with the exception of Mic19, which was depleted in *mic60*Δ (Figure 3A). We conclude that Mic10, Mic12, Mic26, and Mic27 form a stable subcomplex in the absence of Mic19-Mic60.

To analyze the function of the GxGxGxG motifs, we replaced individual glycine residues by alanine. Electron microscopy of $Mic10^{G76A}$ cells revealed alterations of inner membrane

(C) Import of ^{35}S-labeled Mic10 into WT mitochondria. $\Delta\psi$, membrane potential. Precursor, 25% of input.

(D) Protein levels of WT and $Mic10^{K61A,R62A,R63A}$ mitochondria assessed by SDS-PAGE and immunoblotting. μg, total mitochondrial protein.

(E) Representative EM images of mitochondria in WT and $Mic10^{K61A,R62A,R63A}$ cells using DAB staining. Bar, 200 nm.

(F) Subcellular fractionation of WT and $Mic10^{K61A,R62A,R63A}$ yeast. Crude mito., crude mitochondrial fraction; Purif. mito., purified mitochondria.

(G) Left: Mitochondria from WT and $Mic10^{K61A,R62A,R63A}$ cells were analyzed as in (B). Right: Microsomal fractions were treated with proteinase K as indicated and analyzed by SDS-PAGE and immunoblotting.

See also Figure S2.

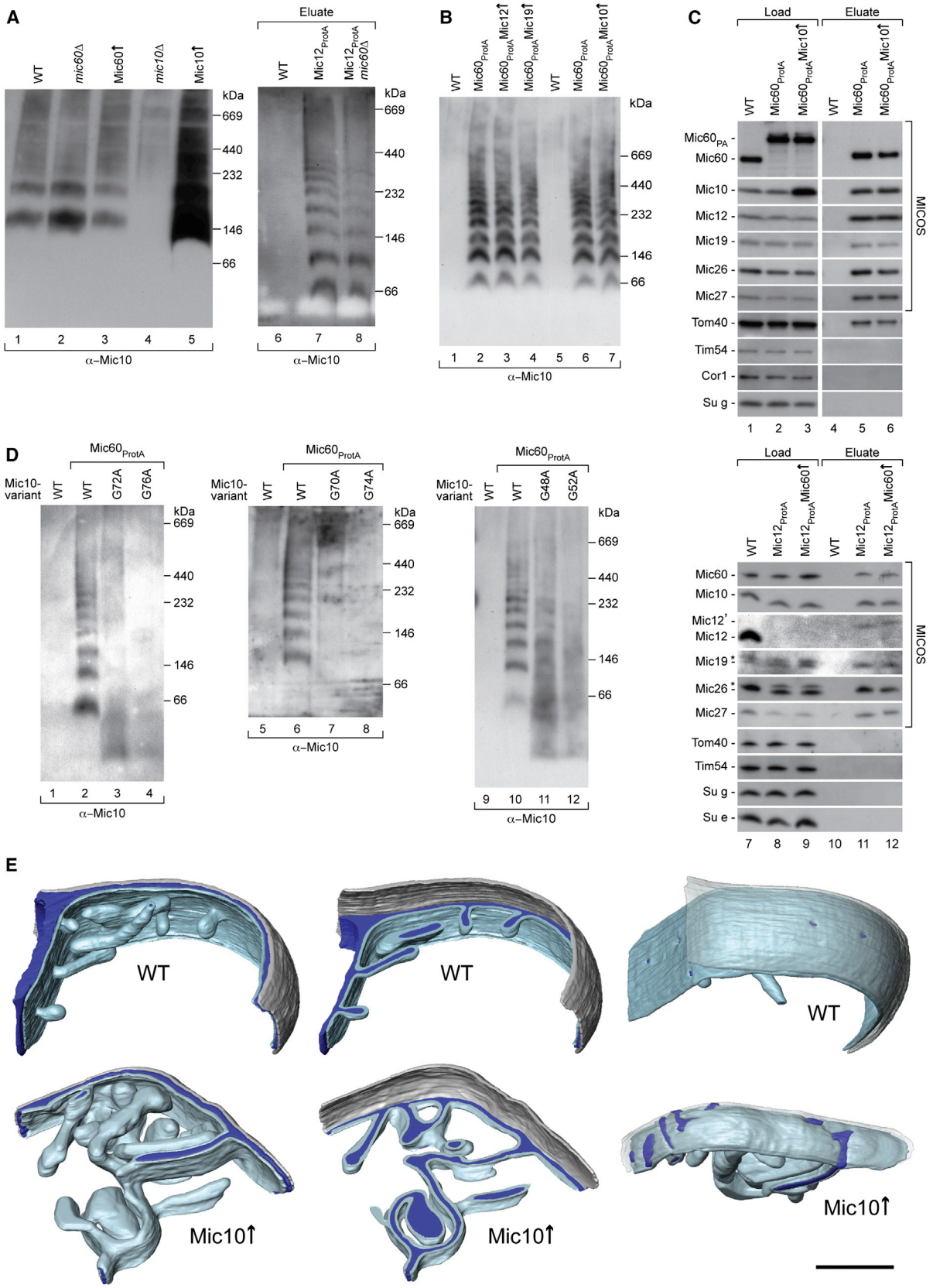

(legend on next page)

architecture with membrane stacks characteristic of *micos* deletion mutants (Figure 3B). Surprisingly, pull-down experiments from Mic10^{G76A} mutant mitochondria yielded a co-purification of all MICOS subunits (Figure 3C, lane 8). We replaced various other glycines in the conserved motifs (glycines 48, 52, 70, 72, 74) by alanine, but did not observe a defective interaction of Mic10 with other MICOS subunits (Figure 3C). Thus, replacement of Mic10 glycine residues disturbs inner membrane architecture, but does not affect the interaction of the different MICOS subunits with each other, suggesting that the glycine motifs and thus Mic10 have an additional role in membrane architecture.

We asked which other function this might be and considered the following points. (1) Harner et al. (2011) reported that Mic10 is considerably more abundant than other MICOS subunits. (2) The subunit c of F_1F_o-ATP synthases is several-fold more abundant than the other ATP synthase subunits (von Ballmoos et al., 2009) and forms homo-oligomers stabilized by the GxGxGxG motif (Vonck et al., 2002; Alavian et al., 2014). (3) We thus speculated that the multiple Mic10 molecules in a MICOS complex may form large oligomers. We purified the MICOS complex via tagged Mic12 or tagged Mic60 from digitonin-lysed mitochondria and analyzed it by blue native electrophoresis. Mic10-specific antibodies indeed decorated a ladder of multiple bands (Figure 3D).

Oligomerization of Mic10 Promotes Formation of Crista Junctions

The high abundance of Mic10 and the characteristic blue native pattern suggest a unique role of Mic10 in the MICOS complex. To study if Mic10 is able to form this pattern by itself, we overexpressed it in yeast under conditions that did not lead to increased levels of other MICOS subunits (Figure 1C) and obtained a surprising result. When digitonin-lysed mitochondria were directly separated on blue native gels, the intensity of the Mic10 ladder increased strongly (Figure 4A, lane 5). However, when the MICOS complex was purified via tagged Mic60 before blue native electrophoresis, the Mic10 ladder was unaffected by the overexpression of Mic10 (Figure 4B, lane 7). We analyzed the composition of the purified MICOS complex and noticed that overexpression of Mic10 led to a considerable increase of the mitochondrial Mic10 levels, but did not change the amount of Mic10 in the MICOS complex; the Mic10 levels in the purified MICOS complex were indistinguishable between wild-type and overexpression mitochondria (Figure 4C). Similarly, overexpression of Mic12, Mic19, or Mic60 increased the levels of these proteins in mitochondria, but not in the purified MICOS complex (Figures 4C and S4A). Thus, the surplus subunits did not co-purify with the MICOS complex, indicating that overexpression of individual subunits does not change the stoichiometry of the MICOS complex. The strong increase in intensity of the blue native ladder of Mic10 upon its overexpression (Figure 4A) supports the view that Mic10 itself forms large oligomers. In line with this view, neither deletion of *MIC60* nor overexpression of Mic12, Mic19, or Mic60 caused substantial alterations of the Mic10 ladder (Figures 4A and 4B).

The conserved GxGxGxG motifs of Mic10 consist of two entwined GxxxG motifs. Helical wheel projections show that GxGxGxG motifs position glycine pairs on opposite sides of an α helix (Figure 2A), thus promoting the stable association of several transmembrane helices. Indeed, the single GxGxGxG motif in the F_1F_o-ATPase subunit c promotes the homo-oligomerization of multiple c subunits into the F_o ring structure (Vonck et al., 2002; Alavian et al., 2014). We speculated that the glycine motifs may be required for homo-oligomerization of Mic10. We asked if replacing of glycines affected the blue native ladder of Mic10. Remarkably, each glycine mutant (glycine 48, 52, 70, 72, 74, or 76 replaced by alanine) strongly disturbed the Mic10 ladder (Figure 4D). Thus, the glycine residues in both transmembrane segments are involved in the formation of stable Mic10 oligomers.

In the double glycine mutant Mic10^{G72A,G76A}, the levels of Mic27 were decreased (Figure S4B). Consistent with the close connection of Mic27 to Mic10, Mic27 was found in a blue native ladder (Figure S4C). Formation of the Mic10 ladder, however, was not blocked by a deletion of *MIC27* (Figure S4D), indicating that Mic27 was not crucial for Mic10 oligomerization. We expressed Mic27 from a high-copy-number plasmid such that its mitochondrial levels were rescued in the Mic10^{G72A,G76A} mutant. The co-purification of Mic10 with Mic60 was influenced neither by replacement of the glycines nor by the level of Mic27 (Figure S4B). The Mic10 ladder was fully dissociated in Mic10^{G72A,G76A} mitochondria independently of the presence or absence of Mic27 (Figure S4E). We conclude that the conserved glycines of Mic10 are not primarily responsible for interaction between different MICOS subunits, but are involved in the formation of Mic10 oligomers.

To examine the ultrastructural consequences of the accumulation of large amounts of Mic10 oligomers in mitochondria, we performed electron cryo-tomography of mitochondria isolated from wild-type and Mic10 overexpression yeast strains. Overexpression of Mic10 led to a considerable increase in the surface area of the inner mitochondrial membrane compared to the wild-type control, resulting in highly interconnected and irregular shaped cristae. These cristae were connected to the inner

Figure 4. Mic10 Oligomers Promote Crista Junction Formation

(A) Left: Mitochondria were solubilized with digitonin and analyzed by blue native PAGE and immunoblotting. Right: Solubilized mitochondria were subjected to IgG affinity chromatography. Elution fractions were analyzed by blue native PAGE.

(B) Mitochondria were used for affinity purification and immunoblotting of elution fractions as in (A).

(C) Mitochondria were subjected to digitonin lysis, IgG affinity chromatography, and SDS-PAGE. Load 4%; eluate 100%. Mic12′, TEV-cleaved Mic12$_{ProtA}$; asterisks, unspecific bands.

(D) WT and Mic60$_{ProtA}$ mitochondria harboring Mic10 variants were analyzed by IgG affinity chromatography and blue native PAGE as in (A).

(E) Segmented surface-rendered representation of a mitochondrion isolated from WT yeast (top) or a Mic10-overexpressing strain (bottom). Left: view from matrix; middle: cut view showing crista junctions; right: view from outer membrane. Gray, outer membrane (transparent in the right panels); light blue, inner membrane; dark blue, intermembrane space (intracristal space in the right panels). Bar, 200 nm. The cristae volume was 1.85% (WT) and 12.2% (Mic10↑) of the volume enclosed by the inner boundary membrane.

See also Figure S4 and Movies S1 and S2.

boundary membrane via multiple slit-like and often branched junctions (Figure 4E; Movies S1 and S2).

We conclude that Mic10 oligomerizes independently of other MICOS subunits through its intrinsic GxGxGxG motifs. Whereas a lack of Mic10 results in a loss of crista junctions, an increased abundance of Mic10 oligomers promotes a massive expansion of crista junctions and deformation of cristae membranes.

Conclusions

Mic10 plays a dual role in the organization of the MICOS complex. It is in close proximity to all other MICOS subunits and forms a core part of a Mic10-12-26-27 subcomplex. In addition, Mic10 forms large oligomers through its characteristic intramembrane GxGxGxG motifs. The conserved glycine motifs promote homotypic interactions of Mic10 and thus drive the formation of large Mic10 oligomers independently of the other MICOS components.

In wild-type mitochondria, the Mic10 oligomers are associated with the MICOS complex. Upon overexpression of Mic10, the levels of other MICOS subunits remain unchanged, and thus Mic10 forms large amounts of oligomers that are not associated with MICOS. The surplus Mic10 oligomers are sufficient to modulate the shape and network architecture of cristae and to expand crista junctions, but do not lead to an increased respiratory activity of mitochondria (Figures S4F–S4H). We propose that Mic10 oligomers form a structural basis of crista junctions; however, the irregular shapes in Mic10 overexpression mitochondria suggest that further components are needed for the proper assembly and organization of crista junctions. Since Mic60 is the second major core component of the MICOS machinery and forms multiple contact sites with the outer membrane, Mic60 may couple a basic Mic10-containing, membrane-shaping structure to the outer membrane, thereby stabilizing and organizing the crista junction structure into the regular appearance seen in wild-type mitochondria. The other MICOS subunits likely play modulatory roles in the formation and maintenance of the MICOS network, yet further work will be needed to define their exact molecular function.

EXPERIMENTAL PROCEDURES

Yeast Growth, Isolation, and Fractionation of Mitochondria

Saccharomyces cerevisiae cells (Table S1) were grown in YPG (1% [w/v] yeast extract, 2% [w/v] peptone, 3% [v/v] glycerol) or synthetic minimal medium (0.67% [w/v] yeast nitrogen base, 0.07% [w/v] CSM amino acid mix, 3% [v/v] glycerol, 0.1% [w/v] glucose). Crude mitochondria were isolated by differential centrifugation and further purified by sucrose gradient centrifugation where indicated. Mitochondria were resuspended in SEM buffer (250 mM sucrose, 1 mM EDTA, 10 mM MOPS [pH 7.2]) and stored at −80°C. For analysis of Mic10 topology and submitochondrial protein localization, mitochondria were diluted 20-fold in hypo-osmotic EM buffer (1 mM EDTA, 10 mM MOPS [pH 7.2]) to selectively permeabilize the outer membrane (hypo-osmotic swelling) and re-isolated by centrifugation. Swollen mitochondria were resuspended in import buffer (3% [w/v] bovine serum albumin, 10 mM MOPS [pH 7.2], 250 mM sucrose, 80 mM KCl, 5 mM $MgCl_2$, 2 mM KH_2PO_4, 5 mM methionine) and treated with proteinase K.

Isolation of Protein Complexes by IgG Affinity Chromatography

Mitochondria isolated from yeast cells expressing protein A fusion constructs and corresponding wild-type strains were solubilized in digitonin buffer (20 mM Tris-HCl [pH 7.4], 50 mM NaCl, 0.1 mM EDTA, 10% [v/v] glycerol, 1% [w/v] digitonin, 2 mM PMSF, 1x EDTA free Protease Inhibitor cocktail [Roche]). Detergent extracts were incubated with IgG-coupled Sepharose beads. After extensive washing, bound proteins were eluted using tobacco etch virus (TEV) protease and samples were subjected to SDS-PAGE or blue native PAGE and immunoblotting.

Electron Microscopy and Electron Cryo-Tomography

Glutaraldehyde-fixed yeast cells were incubated in the presence of diaminobenzidine (DAB) and hydrogen peroxide to visualize cristae membrane domains (von der Malsburg et al., 2011; Zerbes et al., 2012a). For electron cryo-tomography, mitochondrial suspensions were vitrified by plunge-freezing in liquid ethane and imaged on an FEI Polara microscope equipped with energy filter and CCD camera (Quantum, Gatan). Tilt series (± 60°, 1.5° steps) were collected with a specimen pixel size of 6 Å and defocus of 8–9 μm. Tomograms were reconstructed from aligned tilt series using IMOD.

Data Analysis and Statistics

^{35}S-labeled protein bands were detected by digital autoradiography (Storm 865, Storm Imaging System; GE Healthcare) and analyzed using ImageQuant software. In some panels, non-relevant gel lanes were removed by digital image processing and are indicated by white separating lines. Segmentation of tomograms and subsequent movie generation were performed using AMIRA (FEI). For statistical analysis, at least three independent experiments were performed, and the results are represented as mean ± SEM.

SUPPLEMENTAL INFORMATION

Supplemental Information includes Supplemental Experimental Procedures, four figures, one table, and two movies and can be found with this article online at http://dx.doi.org/10.1016/j.cmet.2015.04.007.

ACKNOWLEDGMENTS

We are grateful to Drs. B. Guiard, R. Ieva, A. Reichert, S. Rospert, and N. Wiedemann for discussion and materials and D. Mills for maintenance of the Polara microscope. Work included in this study has also been performed in partial fulfillment of the requirements for the doctoral thesis of R.M.Z. at the University of Freiburg. This work was supported by the Sonderforschungsbereich 746, by the Deutsche Forschungsgemeinschaft (PF 202/8-1), by the Excellence Initiative of the German federal and state governments (EXC 115 CEF Macromolecular Complexes; EXC 294 BIOSS; GSC-4 Spemann Graduate School), by the Max Planck Society, and by postdoctoral fellowships of the Peter and Traudl Engelhorn Stiftung (to H.R.) and the German Academy of Sciences Leopoldina (LPDS 2013-08 to S.E.H.).

Received: December 17, 2014
Revised: March 9, 2015
Accepted: April 1, 2015
Published: May 5, 2015

REFERENCES

Alavian, K.N., Beutner, G., Lazrove, E., Sacchetti, S., Park, H.-A., Licznerski, P., Li, H., Nabili, P., Hockensmith, K., Graham, M., et al. (2014). An uncoupling channel within the c-subunit ring of the F_1F_O ATP synthase is the mitochondrial permeability transition pore. Proc. Natl. Acad. Sci. USA *111*, 10580–10585.

Alkhaja, A.K., Jans, D.C., Nikolov, M., Vukotic, M., Lytovchenko, O., Ludewig, F., Schliebs, W., Riedel, D., Urlaub, H., Jakobs, S., and Deckers, M. (2012). MINOS1 is a conserved component of mitofilin complexes and required for mitochondrial function and cristae organization. Mol. Biol. Cell *23*, 247–257.

Bohnert, M., Wenz, L.-S., Zerbes, R.M., Horvath, S.E., Stroud, D.A., von der Malsburg, K., Müller, J.M., Oeljeklaus, S., Perschil, I., Warscheid, B., et al. (2012). Role of mitochondrial inner membrane organizing system in protein biogenesis of the mitochondrial outer membrane. Mol. Biol. Cell *23*, 3948–3956.

Darshi, M., Mendiola, V.L., Mackey, M.R., Murphy, A.N., Koller, A., Perkins, G.A., Ellisman, M.H., and Taylor, S.S. (2011). ChChd3, an inner mitochondrial

membrane protein, is essential for maintaining crista integrity and mitochondrial function. J. Biol. Chem. *286*, 2918–2932.

Davies, K.M., Anselmi, C., Wittig, I., Faraldo-Gómez, J.D., and Kühlbrandt, W. (2012). Structure of the yeast F_1F_o-ATP synthase dimer and its role in shaping the mitochondrial cristae. Proc. Natl. Acad. Sci. USA *109*, 13602–13607.

Frey, T.G., and Mannella, C.A. (2000). The internal structure of mitochondria. Trends Biochem. Sci. *25*, 319–324.

Frezza, C., Cipolat, S., Martins de Brito, O., Micaroni, M., Beznoussenko, G.V., Rudka, T., Bartoli, D., Polishuck, R.S., Danial, N.N., De Strooper, B., and Scorrano, L. (2006). OPA1 controls apoptotic cristae remodeling independently from mitochondrial fusion. Cell *126*, 177–189.

Harner, M., Körner, C., Walther, D., Mokranjac, D., Kaesmacher, J., Welsch, U., Griffith, J., Mann, M., Reggiori, F., and Neupert, W. (2011). The mitochondrial contact site complex, a determinant of mitochondrial architecture. EMBO J. *30*, 4356–4370.

Head, B.P., Zulaika, M., Ryazantsev, S., and van der Bliek, A.M. (2011). A novel mitochondrial outer membrane protein, MOMA-1, that affects cristae morphology in *Caenorhabditis elegans*. Mol. Biol. Cell *22*, 831–841.

Hoppins, S., Collins, S.R., Cassidy-Stone, A., Hummel, E., Devay, R.M., Lackner, L.L., Westermann, B., Schuldiner, M., Weissman, J.S., and Nunnari, J. (2011). A mitochondrial-focused genetic interaction map reveals a scaffold-like complex required for inner membrane organization in mitochondria. J. Cell Biol. *195*, 323–340.

Jans, D.C., Wurm, C.A., Riedel, D., Wenzel, D., Stagge, F., Deckers, M., Rehling, P., and Jakobs, S. (2013). STED super-resolution microscopy reveals an array of MINOS clusters along human mitochondria. Proc. Natl. Acad. Sci. USA *110*, 8936–8941.

John, G.B., Shang, Y., Li, L., Renken, C., Mannella, C.A., Selker, J.M.L., Rangell, L., Bennett, M.J., and Zha, J. (2005). The mitochondrial inner membrane protein mitofilin controls cristae morphology. Mol. Biol. Cell *16*, 1543–1554.

Körner, C., Barrera, M., Dukanovic, J., Eydt, K., Harner, M., Rabl, R., Vogel, F., Rapaport, D., Neupert, W., and Reichert, A.S. (2012). The C-terminal domain of Fcj1 is required for formation of crista junctions and interacts with the TOB/SAM complex in mitochondria. Mol. Biol. Cell *23*, 2143–2155.

Meeusen, S., DeVay, R., Block, J., Cassidy-Stone, A., Wayson, S., McCaffery, J.M., and Nunnari, J. (2006). Mitochondrial inner-membrane fusion and crista maintenance requires the dynamin-related GTPase Mgm1. Cell *127*, 383–395.

Merkwirth, C., Dargazanli, S., Tatsuta, T., Geimer, S., Löwer, B., Wunderlich, F.T., von Kleist-Retzow, J.C., Waisman, A., Westermann, B., and Langer, T. (2008). Prohibitins control cell proliferation and apoptosis by regulating OPA1-dependent cristae morphogenesis in mitochondria. Genes Dev. *22*, 476–488.

Mun, J.Y., Lee, T.H.L., Kim, J.H., Yoo, B.H., Bahk, Y.Y., Koo, H.-S., and Han, S.S. (2010). *Caenorhabditis elegans* mitofilin homologs control the morphology of mitochondrial cristae and influence reproduction and physiology. J. Cell. Physiol. *224*, 748–756.

Ott, C., Ross, K., Straub, S., Thiede, B., Götz, M., Goosmann, C., Krischke, M., Mueller, M.J., Krohne, G., Rudel, T., and Kozjak-Pavlovic, V. (2012). Sam50 functions in mitochondrial intermembrane space bridging and biogenesis of respiratory complexes. Mol. Cell. Biol. *32*, 1173–1188.

Paumard, P., Vaillier, J., Coulary, B., Schaeffer, J., Soubannier, V., Mueller, D.M., Brèthes, D., di Rago, J.-P., and Velours, J. (2002). The ATP synthase is involved in generating mitochondrial cristae morphology. EMBO J. *21*, 221–230.

Pfanner, N., van der Laan, M., Amati, P., Capaldi, R.A., Caudy, A.A., Chacinska, A., Darshi, M., Deckers, M., Hoppins, S., Icho, T., et al. (2014). Uniform nomenclature for the mitochondrial contact site and cristae organizing system. J. Cell Biol. *204*, 1083–1086.

Rabl, R., Soubannier, V., Scholz, R., Vogel, F., Mendl, N., Vasiljev-Neumeyer, A., Körner, C., Jagasia, R., Keil, T., Baumeister, W., et al. (2009). Formation of cristae and crista junctions in mitochondria depends on antagonism between Fcj1 and Su *e/g*. J. Cell Biol. *185*, 1047–1063.

Russ, W.P., and Engelman, D.M. (2000). The GxxxG motif: a framework for transmembrane helix-helix association. J. Mol. Biol. *296*, 911–919.

Senes, A., Engel, D.E., and DeGrado, W.F. (2004). Folding of helical membrane proteins: the role of polar, GxxxG-like and proline motifs. Curr. Opin. Struct. Biol. *14*, 465–479.

Strauss, M., Hofhaus, G., Schröder, R.R., and Kühlbrandt, W. (2008). Dimer ribbons of ATP synthase shape the inner mitochondrial membrane. EMBO J. *27*, 1154–1160.

van der Laan, M., Bohnert, M., Wiedemann, N., and Pfanner, N. (2012). Role of MINOS in mitochondrial membrane architecture and biogenesis. Trends Cell Biol. *22*, 185–192.

Vogel, F., Bornhövd, C., Neupert, W., and Reichert, A.S. (2006). Dynamic subcompartmentalization of the mitochondrial inner membrane. J. Cell Biol. *175*, 237–247.

von Ballmoos, C., Wiedenmann, A., and Dimroth, P. (2009). Essentials for ATP synthesis by F_1F_0 ATP synthases. Annu. Rev. Biochem. *78*, 649–672.

von der Malsburg, K., Müller, J.M., Bohnert, M., Oeljeklaus, S., Kwiatkowska, P., Becker, T., Loniewska-Lwowska, A., Wiese, S., Rao, S., Milenkovic, D., et al. (2011). Dual role of mitofilin in mitochondrial membrane organization and protein biogenesis. Dev. Cell *21*, 694–707.

Vonck, J., von Nidda, T.K., Meier, T., Matthey, U., Mills, D.J., Kühlbrandt, W., and Dimroth, P. (2002). Molecular architecture of the undecameric rotor of a bacterial Na^+-ATP synthase. J. Mol. Biol. *321*, 307–316.

Weber, T.A., Koob, S., Heide, H., Wittig, I., Head, B., van der Bliek, A., Brandt, U., Mittelbronn, M., and Reichert, A.S. (2013). APOOL is a cardiolipin-binding constituent of the Mitofilin/MINOS protein complex determining cristae morphology in mammalian mitochondria. PLoS ONE *8*, e63683.

Xie, J., Marusich, M.F., Souda, P., Whitelegge, J., and Capaldi, R.A. (2007). The mitochondrial inner membrane protein mitofilin exists as a complex with SAM50, metaxins 1 and 2, coiled-coil-helix coiled-coil-helix domain-containing protein 3 and 6 and DnaJC11. FEBS Lett. *581*, 3545–3549.

Zerbes, R.M., Bohnert, M., Stroud, D.A., von der Malsburg, K., Kram, A., Oeljeklaus, S., Warscheid, B., Becker, T., Wiedemann, N., Veenhuis, M., et al. (2012a). Role of MINOS in mitochondrial membrane architecture: cristae morphology and outer membrane interactions differentially depend on mitofilin domains. J. Mol. Biol. *422*, 183–191.

Zerbes, R.M., van der Klei, I.J., Veenhuis, M., Pfanner, N., van der Laan, M., and Bohnert, M. (2012b). Mitofilin complexes: conserved organizers of mitochondrial membrane architecture. Biol. Chem. *393*, 1247–1261.

Zick, M., Rabl, R., and Reichert, A.S. (2009). Cristae formation-linking ultrastructure and function of mitochondria. Biochim. Biophys. Acta *1793*, 5–19.